2014-11-17

Doping dependence and anisotropy of minority electron mobility in molecular beam epitaxy-grown p type GaInP

Haegel, N. M.

American Institute of Physics

Doping dependence and anisotropy of minority electron mobility in molecular beam epitaxy-grown p type GaInP

N. M. Haegel,[1] T. Christian,[1] C. Scandrett,[2] A. G. Norman,[1] A. Mascarenhas,[1] Pranob Misra,[3] Ting Liu,[3] Arsen Sukiasyan,[3] Evan Pickett,[3] and Homan Yuen[3]
[1]*National Renewable Energy Laboratory, Golden, Colorado 80401, USA*
[2]*Naval Postgraduate School, Monterey, California 93943, USA*
[3]*Solar Junction, Inc., San Jose, California 95131, USA*

(Received 21 October 2014; accepted 8 November 2014; published online 21 November 2014)

Direct imaging of minority electron transport via the spatially resolved recombination luminescence signature has been used to determine carrier diffusion lengths in GaInP as a function of doping. Minority electron mobility values are determined by performing time resolved photoluminescence measurements of carrier lifetime on the same samples. Values at 300 K vary from ~2000 to 400 $cm^2/V\,s$ and decrease with increasing doping. Anisotropic diffusion lengths and strongly polarized photoluminescence are observed, resulting from lateral composition modulation along the [110] direction. We report anisotropic mobility values associated with carrier transport parallel and perpendicular to the modulation direction.
 [http://dx.doi.org/10.1063/1.4902316]

Gallium indium phosphide (GaInP) is a ternary semiconductor alloy, routinely used as the largest bandgap top cell in multijunction solar cells, as well as in GaAs heterojunction bipolar transistors and a variety of heterojunction nanostructures. Despite the longstanding use of this material in solar cells, where minority carrier transport plays a fundamental role, experimental values for minority carrier mobility are very limited. Majority carrier mobility can be routinely determined through Hall effect measurements, but minority carrier transport parameters such as diffusion length and mobility are generally extracted through analysis of device performance. For optimized device modeling, however, it is valuable to have direct experimental values, particularly of the minority carrier mobility. While minority carrier lifetime generally reflects significant variations in individual material quality and growth conditions, the mobility is a more fundamental parameter, dependent primarily on doping and lattice temperature.

We have made direct measurements of minority electron diffusion lengths L_d at 300 K as a function of doping in p type $Ga_{0.5}In_{0.5}P$, over a doping range from 5×10^{16} to $1 \times 10^{18}\,cm^{-3}$. Diffusion lengths were measured via transport imaging in a scanning electron microscope (SEM) by mapping the spatial variation of the luminescence produced when excess carriers are generated in a fixed location by an electron beam. The samples are placed in the SEM; the electron beam passes through a small hole in the optical microscope reflecting surface. The electron beam is held at a fixed point, creating a quasi-point source for generation of excess carriers. The resulting luminescence is collected with an optical microscope and detected by a thermoelectrically cooled Apogee Alta CCD camera, with pixels of dimension 6.8 $\mu m \times 6.8\,\mu m$. The magnification is 40×, resulting in an image scale of 0.4 μm/pixel. The CCD exposure time can be varied, depending on the luminescent intensity. This transport imaging approach in the SEM has been described in detail in earlier work.[1,2]

Excess carriers created at a point will diffuse and some fraction will recombine along the way, over a characteristic distance given by the minority carrier diffusion length. By maintaining the spatial information in the recombination luminescence, L_d can be obtained directly from the optical image. In this regard, transport imaging is different than scanning cathodoluminescence or photoluminescence, where spatial information about the sample is obtained by scanning the excitation point and assuming that all luminescence is associated with the point of generation. Transport imaging takes advantage of the fact that the resulting luminescence is actually distributed about the point of origin.

The samples are double heterostructures of GaInP, with $Al_{0.25}Ga_{0.25}In_{0.5}P$ barriers. The substrate is [001] semi-insulating GaAs. The GaInP layers were grown by molecular beam epitaxy (MBE), with an MBE-grown GaAs buffer layer. The GaInP layers for all samples were 333 nm thick, with $Al_{0.25}Ga_{0.25}In_{0.5}P$ barrier layers of thickness 50 nm (top) and 200 nm (bottom). Cathodoluminescence and photoluminescence spectroscopy both indicate that the only significant luminescence signal is from the GaInP layer. Samples were doped p type using Be. Doping level calibration was performed by Hall effect on layers grown under similar conditions. Transport imaging measurements were performed on both as-grown and rapid thermal annealed samples. For these samples, the electron beam excitation energy was 5 kV, with a probe current of 3×10^{-11} A. Exposure times for the optical images, which vary primarily due to the variations in doping, ranged from 0.1 to 1 s.

Figure 1 shows examples of the spatially resolved luminescence images for the as-grown and annealed samples for the lowest and highest doping levels. One sees the evidence for the anisotropic transport most clearly in the $5 \times 10^{16}\,cm^{-3}$ doped material, indicated by the oval shape of the luminescence distribution. Other samples show varying degrees of anisotropy. The axis of highest diffusion length is located along the [−1 1 0] crystallographic axis, as indicated in the inset of Figure 1.

The value for L_d is determined by a least squares numerical fit to the intensity profile $I(r)$ along any axis, taking the origin as the center of the excitation spot. In the low injection regime ($p_{excess} \approx n_{excess} \ll p_{doping}$), the intensities in the

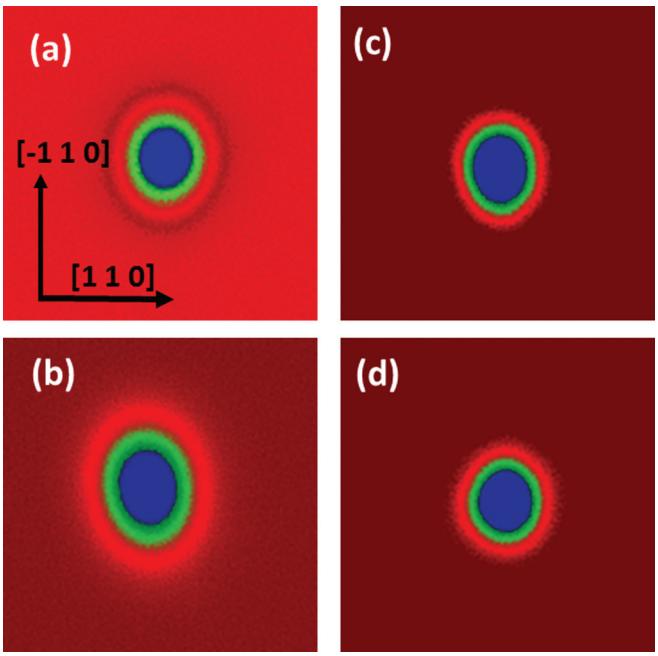

FIG. 1. Optical images (false color) indicating GaInP luminescence distribution as a function of position in response to point source excitation for doping of (a) $5 \times 10^{16}\,cm^{-3}$ (as grown), (b) $5 \times 10^{16}\,cm^{-3}$ (annealed), (c) $1 \times 10^{18}\,cm^{-3}$ (as grown), and (d) $1 \times 10^{18}\,cm^{-3}$ (annealed). Electron beam spot excitation was at 5 keV and a probe current of 3×10^{-11} A. Image dimensions in all cases are 50 μm × 50 μm.

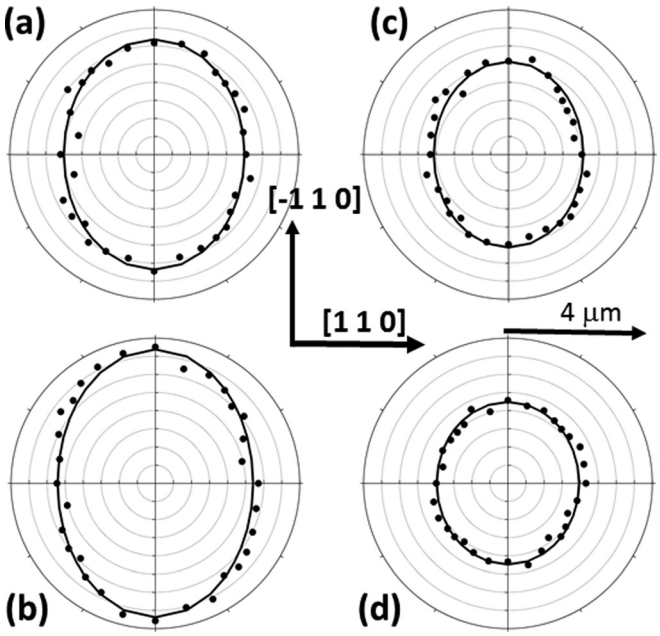

FIG. 2. Extracted L_d values as a function of angle for the images shown in Figure 1. In all cases, the radial axis has a maximum length of 4 μm. Anisotropy is most apparent in samples (a) and (b).

optical images are assumed to be proportional to the minority-carrier concentration within the heterostructure. For the electron beam excitation used here, we estimate the excess carrier population to be $\sim 3 \times 10^{14}\,cm^{-3}$, well within the low injection regime since the majority doping levels of interest are in the range of 10^{16}–$10^{18}\,cm^{-3}$. In this case, the minority carrier population can be modeled by a two-dimensional diffusion equation with source and recombination terms.[1] The asymptotic solution, for the region starting at a small distance (≥ 4 μm) from the origin is

$$I(r) \sim \left(\frac{g}{2\pi D}\right) Ko\left(\frac{r}{L_d}\right) + B, \qquad (1)$$

where I is the intensity, g is the source term amplitude, D is the minority carrier diffusivity, B is the background term, L_d is the minority carrier diffusion length, and r is the distance from the excitation point. Data subsets are extracted along 32 different angles and for each of the subsets a "best fit" value for L_d is found employing a least squares analysis. The angles are chosen to align with a rectangular grid so there is no interpolation of intensities employed in fitting data to asymptotic curves. The corresponding polar plots for L_d as a function of direction are shown in Figure 2 for the images in Figure 1. The 32 values of L_d at varying angles are in turn "fit" to an ellipse using the fact that the total distance from any point on an ellipse to its two foci is the constant length 2a, where a is the semi-major axis length. The semi-minor axis b is found from the determination of the semi-major axis length and coordinates of the foci. The foci coordinates and the value of "a" are the five undetermined values used in a least squares fit to the data.

The variations in L_d associated with the material anisotropy are 25% and 31% ($5 \times 10^{16}\,cm^{-3}$ as grown and annealed) and 19% and 9.5% ($1 \times 10^{18}\,cm^{-3}$ as grown and annealed), respectively, for these four cases, taking the difference in L_d along the major and minor axes of the transport distribution and dividing by the average value.

While the minority carrier diffusion lengths are of interest in device performance, they are fundamentally determined by two important parameters, the minority carrier lifetime τ and mobility μ, since $L_d = ((kT/e)\ \mu\tau)^{1/2}$. With an independent measurement of the minority carrier lifetime, therefore, the L_d values can be used to obtain a direct measurement of the minority carrier mobility—in this case, as a function of doping in room temperature GaInP. Earlier published experimental values for minority carrier mobility are limited to a single doping value.[1]

Time resolved photoluminescence (TRPL) measurements to determine minority carrier lifetime τ were performed using a pulsed, tunable titanium-sapphire laser with pulse lengths of ~150 fs. The laser output was frequency doubled to produce pulses at 405 nm. Luminescence was collected with a streak camera. The deposited energy per pulse was approximately 7 nJ/cm^2, resulting in a minority carrier population density of $\sim 5 \times 10^{14}\,cm^{-3}$. Consistent with the electron beam measurements, this places us in the low injection regime. This is important for the determination of an accurate mobility, since the lifetime becomes excitation dependent at higher excitation levels.

The diffusion length and TRPL results for all samples—four doping levels with as-grown and annealed conditions in all cases—are summarized in Table I. The luminescence decay times are relatively short and insensitive to doping, consistent with dominant non-radiative recombination in the low-level excitation conditions used here. Tabulated TRPL measurements were conducted without specific polarization

TABLE I. TRPL, minority carrier diffusion lengths and resultant minority carrier mobilities, as-grown and annealed. All results are for 300 K.

	As grown					Annealed				
Doping (cm^{-3})	Lifetime (ns)	L_d (μm) major	L_d (μm) minor	μ major cm^2/V s	μ minor cm^2/V s	Lifetime (ns)	L_d (μm) major	L_d (μm) minor	μ major cm^2/V s	μ minor cm^2/V s
5×10^{16}	2.5	3.2	2.5	1580	962	3.4	3.7	2.7	1550	825
1×10^{17}	2.8	3.0	2.4	1240	791	5.3	3.9	3.1	1100	697
5×10^{17}	3.2	2.5	1.9	751	434	4.5	3.0	2.35	769	472
1×10^{18}	4.0	2.55	2.1	625	424	2.9	2.0	2.0	642	531

analysis. In all but the most heavily doped case, annealing results in an increase in minority carrier lifetime. Diffusion lengths, which range from ~2 to 4 μm in all cases, also increase with annealing, except in the most heavily doped case. Discussion of diffusion length in these materials must now take into account the anisotropy. The largest fractional anisotropy in L_d among these materials, as previously defined, is 31% for the annealed sample with doping of $5 \times 10^{16}\,cm^{-3}$.

Combining the L_d and τ values, we determine the minority carrier mobilities—electron mobilities in p type material—as a function of doping. Results are shown in Figure 3. We see a decreasing mobility as a function of doping over the range of study, typical of majority carrier mobility trends in many other semiconductor materials.[3] It is important to note the consistency in the mobility data (two samples of each type for reproducibility, as well as the as-grown and annealed conditions). Annealing, generally, causes variations in minority carrier lifetime due to improvement of material quality caused by thermal processes. That is why fundamental mobility values are routinely tabulated for semiconductor materials, while fundamental lifetime values refer to a radiative limit that is often not realized. The reproducibility on the mobility values, despite the variations in L_d and τ as a function of annealing, is a good indication of the quality of the data for both L_d and τ in the low injection regime.

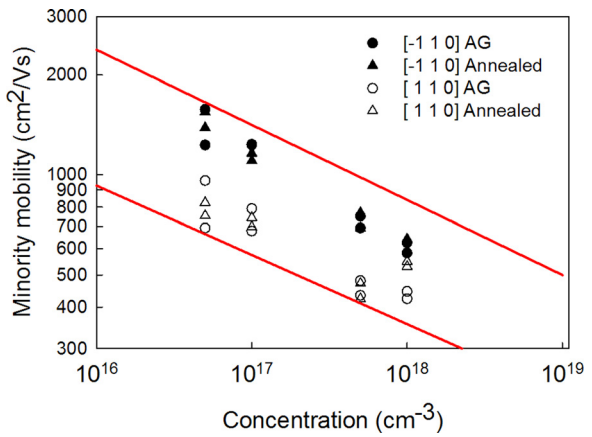

FIG. 3. Minority electron mobility (300 K) as a function of doping. Two samples were measured in each case for reproducibility. Filled symbols are mobility values along the major axis and open symbols are mobility values along the minor axis. The red (solid) lines indicate the range of values in the literature for majority electron mobility (300 K) as a function of doping in GaInP with ~50/50% Ga/In composition [Majority mobility ranges taken from Refs. 4–7.]

We note that the analysis of the spatial luminescence data assumes low surface recombination velocity at the heterostructure interfaces. There is evidence for this from the excellent fit to Eq. (1). However, even if interface recombination affects the lifetime, it will have a similar effect on the TRPL results and therefore should not affect the extracted values for mobility.

To compare the minority electron mobilities in p type GaInP to majority electron mobilities in n type materials of comparable doping, we reviewed the literature for majority electron mobility data in GaInP.[4–7] There is significant scatter in the reported data, perhaps reflecting variations in the type of growth and sample quality, as well as uncertainties in the doping. The red lines in Figure 3 span the range of values reported as a function of doping. One sees that the minority mobilities reported here fall within the same general range. In GaAs, theoretical work suggests that minority electron mobilities at room temperature are slightly lower than majority electron mobilities, due to primarily the scattering behavior associated with heavy holes.[8] However, in GaInP, additional factors, such as alloy scattering or the formation of microdomains,[9] may play a significant role in limiting the mobility for both types of carriers. Temperature dependent measurements of the minority carrier mobility in GaInP have shown a strong deviation from majority mobility behavior.[2]

The observation of the strong transport anisotropy in MBE-grown GaInP raises obvious questions as to its origin. Two possibilities are Cu-Pt ordering, which has previously been shown to produce transport anisotropy in GaInP,[1,10] and compositional modulation.[11,12] Although commonly observed at the higher temperatures associated with metalorganic chemical vapor deposition (MOCVD) growth, Cu-Pt ordering has also been observed in solid source MBE-grown material.[13] In order to investigate which phenomenon is dominant in this case, variable temperature polarized photoluminescence studies were performed. For these studies, an R6G tunable dye laser was used to excite photoluminescence, and a half-wave plate combined with a polarization analyzer was used to detect luminescence polarized along each crystallographic axis, [−1 1 0] and [1 1 0].

Figure 4 shows representative polarized photoluminescence spectra from such a measurement on an annealed sample with $5 \times 10^{16}\,cm^{-3}$ doping level. For these studies, an R6G dye laser tuned to 620 nm was used to excite photoluminescence and the excitation power density was approximately $10\,W/cm^2$. Each spectrum consists of two peaks. The high-energy peak is present in both polarization analysis directions and consistent with PL emission from bulk GaInP,

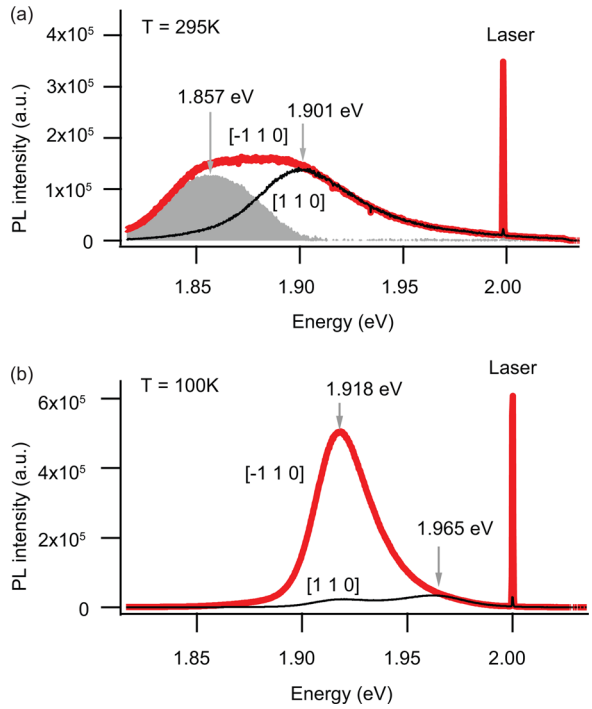

FIG. 4. Example of polarized photoluminescence from the annealed sample with p-type doping 5×10^{16} cm^3 at (a) 295 K and (b) 100 K. Photoluminescence polarization is analyzed along either the [1 1 0] (black, thin line) or [−1 1 0] (red, thick line) crystallographic axes. Laser excitation is approximately 40 W/cm^2 at 2.00 eV, polarized along the [−1 1 0] axis. The shaded area in (a) illustrates a direct subtraction of the two polarized PL traces to highlight the lower energy peak.

while the low-energy peak is red-shifted by approximately 45 meV and is strongly polarized along the [−1 1 0] direction. The polarization ratio of the low energy peak, defined in terms of the intensity at the peak energy as $\rho = (I_{[-1\ 1\ 0]} - I_{[1\ 1\ 0]})/(I_{[-1\ 1\ 0]} + I_{[1\ 1\ 0]})$, is $\rho = 0.71$ at 295 K and $\rho = 0.91$ at 100 K. The luminescence anisotropy was independent of laser polarization orientation. The two spectral peaks are attributed to emission from spatially distinct regions within the GaInP active layer. The TRPL decay times at 295 K were consistent across the full range of spectral energies in both polarization orientations, suggesting that carriers are thermally exchanged between these regions.

The observed strong anisotropy in optical transitions is strongly suggestive of composition modulation along the [1 1 0] direction. This type of composition modulation occurs regularly in strained short-period superlattices of III-V alloys[14] and has also been observed to arise spontaneously in MOCVD-grown alloys.[11,15,16] The polarization ratios measured here greatly exceed even the theoretical maximum of 0.5 that could occur for perfectly atomically ordered material (see, e.g., Ref. 17).

Cross sectional transmission electron microscopy (TEM) on the as-grown 5×10^{16} cm^{-3} doped sample confirms the presence of compositional modulation. Figure 5 shows strong lateral composition modulation along [110] in a [−1 1 0] cross section in both strain sensitive (220) and chemically sensitive (002) dark field images. The modulation in alloy composition along the [1 1 0] direction would contribute to increased carrier scattering for motion in that direction, explaining the observed diffusion anisotropy.

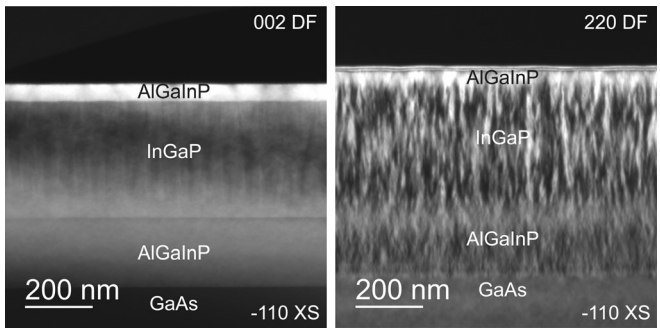

FIG. 5. Chemically sensitive (left) and strain sensitive (right) cross sectional TEM images showing compositional modulation. Lateral compositional modulation is seen along the [110] direction in a [−1 1 0] cross section.

In summary, we used a combination of transport imaging and TRPL to determine minority carrier electron mobility in GaInP as a function of p type doping over the range from 5×10^{16} cm^{-3} to 1×10^{18} cm^{-3}. Room temperature mobility values range from ~400 to 2000 cm^2/V s and show decreasing mobility as a function of doping. Transport anisotropy, associated with compositional modulation along the [110] direction, is observed in many of the samples. The experimental data for minority carrier mobility should be of value in improved modeling and simulation for a range of devices, including the highest efficiency multijunction solar cells that utilize GaInP alloys.

This work was supported at the Naval Postgraduate School in part by National Science Foundation Grant No. DMR-0804527 and in part by the NPS Energy Academic Group with funding from the Navy Energy Coordination Office. T.C. acknowledges support from the Department of Energy, Office of Science Graduate Fellowship Program (DOE SCGF), made possible in part by the American Recovery and Reinvestment Act of 2009, administered by ORISE-ORAU under Control No. DE-AC05-06OR23100. TRPL work at NREL was supported by the Department of Energy Office of Science, Basic Energy Sciences under DEAC36-08GO28308.

[1]N. M. Haegel, T. J. Mills, M. Talmadge, C. Scandrett, C. Frenzen, H. J. Yoon, C. Fetzer, and R. King, J. Appl. Phys. **105**, 023711 (2009).
[2]F. J. Schultes, T. Christian, R. Jones-Albertus, E. Pickett, K. Alberi, B. Fluegel, T. Liu, P. Misra, A. Sukiasyan, H. Yuen, and N. M. Haegel, Appl. Phys. Lett. **103**, 242106 (2013).
[3]S. Sze and K. Ng, *Physics of Semiconductor Devices*, 3rd ed. (Wiley, New York, 2007).
[4]T. Shitara and K. Eberl, Appl. Phys. Lett. **65**, 356 (1994) and references therein.
[5]Z. Z. Sun, S. F. Yoon, and W. K. Loke, J. Cryst. Growth **235**, 8 (2002).
[6]B. R. Nag and M. Das, J. Appl. Phys. **83**, 5862 (1998).
[7]R. Jakomin, A. Parasini, L. Tarricone, M. Longo, B. Fraboni, and S. Vantaggio, Thin Solid Films **520**, 6619 (2012).
[8]W. Walukiewicz, J. Lagowski, L. Jastrezebski, and H. C. Gatos, J. Appl. Phys. **50**, 5040 (1979).
[9]D. J. Friedman, A. E. Kibbler, and J. M. Olson, Appl. Phys. Lett. **59**, 2998 (1991).
[10]P. Ernst, Y. Zhang, F. A. J. M. Driessen, A. Mascarenhas, E. D. Jones, C. Geng, F. Scholz, and H. Schweizer, J. Appl. Phys. **81**, 2814 (1997).
[11]C. M. Fetzer, R. T. Lee, S. W. Jun, G. B. Stringfellow, S. M. Lee, and T. Y. Seong, Appl. Phys. Lett. **78**, 1376 (2001).
[12]Y. Q. Wang, Z. L. Wang, T. Brown, A. Brown, and G. May, J. Electron. Mater. **29**, 1372 (2000).

[13]S. F. Yoon, K. W. Mah, H. Q. Xheng, B. P. Gay, and P. H. Zhang, Microelectron. J. **31**, 15 (2000).
[14]J. Mirecki Millunchick, R. D. Twesten, S. R. Lee, D. M. Follstaedt, E. D. Jones, S. P. Ahrenkiel, Y. Zhang, and A. Mascarenhas, MRS Bull. **22**(7), 38 (1997).
[15]S. W. Jun, T.-Y. Seong, J. H. Lee, and B. Lee, Appl. Phys. Lett. **68**, 3443 (1996).
[16]S. Francoeur, M. C. Hanna, A. G. Norman, and A. Mascarenhas, Appl. Phys. Lett. **80**, 243 (2002).
[17]S. H. Wei and A. Zunger, Appl. Phys. Lett. **64**, 1676 (1994).